Graefes Arch Clin Exp Ophthalmol (2015) 253:865–874
DOI 10.1007/s00417-014-2917-7

BASIC SCIENCE

Regulation of surface expression of TRPV2 channels in the retinal pigment epithelium

Nadine Reichhart · Susanne Keckeis · Frederik Fried · Gabriele Fels · Olaf Strauss

Received: 7 October 2014 / Revised: 23 December 2014 / Accepted: 23 December 2014 / Published online: 24 January 2015

Abstract
Purpose The retinal pigment epithelium (RPE) interacts closely with the photoreceptors in fulfilling tasks of visual function. Since an understanding of the RPE function is essential for understanding the patho-mechanisms involved in vision loss, we explored the regulation of the vanilloid receptor subtype transient receptor potential TRPV2 channels that trigger insulin-like growth factor-1 (IGF-1)-induced vascular endothelial growth factor A (VEGF-A) secretion.
Methods Immunohistochemistry was used to assess TRPV2 expression in retinal cross-sections or ARPE-19 cells, and surface expression of TRPV2 was quantified using confocal microscopy. Membrane currents of ARPE-19 cells were recorded using a whole-cell configuration of the patch-clamp technique.
Results TRPV2 expression was detected in the RPE of the mouse retina as well as in ARPE-19 cells. Increasing the temperature to 45 °C activated membrane conductance sensitive to SKF-96365 and ruthenium red in 60 % of cells. Preincubation with either cannabidiol (CBD) or IGF-1 led to a three- or fourfold increase in current density, respectively, in all cells, which was blocked by SKF-96365. In contrast to IGF-1, CBD stimulation of membrane conductance was further increased by heat. TRPV2 surface expression was increased by both IGF-1 and CBD, with the increase by CBD twice as large as that by IGF-1. The phosphatidylinositol 3-kinase (PI3K) inhibitor LY294002 abolished the effects on membrane conductance and surface expression.
Conclusions Both CBD and IGF-1 enhance TRPV2 channel activity by specific proportions of both channel activation and PI 3-kinase-dependent surface expression: IGF-1 predominantly increases ion channel activity, whereas CBD is more active in increasing TRPV2 surface expression. Thus, differential regulation of TRPV2 surface expression is an important mechanism for modulating the responsiveness of the RPE to growth factors.

Keywords TRPV2 · Surface expression · CBD · IGF-1 · VEGF · RPE

N. Reichhart · S. Keckeis · F. Fried · G. Fels · O. Strauss (✉)
Experimental Ophthalmology, Department of Ophthalmology, Campus Virchow Clinics, Charité University Medicine Berlin, Augustenburger Platz 1, 13353 Berlin, Germany
e-mail: olaf.strauss@charite.de

Introduction

The retinal pigment epithelium (RPE) forms a portion of the blood/retina barrier [1–4] and is a closely interacting partner with the photoreceptors in the retina. From this synergy, the RPE fulfills a variety of tasks that are essential for visual function [1, 4, 5]. A loss or alteration in RPE function is involved in a variety of retinal degenerative conditions, including age-related macular degeneration (AMD) [6, 7] and retinitis pigmentosa [8, 9]. Thus, an understanding of the regulation of RPE function in health and disease is essential for understanding the mechanisms of retinal degeneration and for developing therapeutic targets.

One of the most important functions of the RPE is the secretion of a variety of growth factors, among which are vascular endothelial growth factor A ((VEGF-A), which acts to stabilize the fenestrated endothelium of the choriocapillaris [5, 10–12], and pigment epithelium-derived factor (PEDF), which helps to maintain the structural integrity of the photoreceptors [5, 13–15]. In disease, the regulation of growth factor secretion can change. For example, increased secretion of VEGF-A by the RPE has been implicated in choroidal neovascularization that occurs in AMD [5, 7, 12, 16, 17]. Several mechanisms can cause an increase in VEGF-A secretion, including autocrine or paracrine stimulation of the RPE by

fibroblast growth factors [5, 18–20], by VEGF isoforms [21], and by insulin-like growth factor-1 (IGF-1) [22–26]. The release of VEGF-A by the RPE cells is triggered by the activity of various types of Ca^{2+} channels [5, 16, 19, 20, 27].

An important regulator of RPE function is the transient receptor potential vanilloid 2 subtype (TRPV2) Ca^{2+}-conducting ion channel [22]. This channel belongs to the group of temperature-sensitive channels of the TRP ion channel family, and it is activated by increases in temperature to values above 45 °C [22, 28–30]. Cordeiro et al. showed that although the mRNA of TRPV1–4 can be detected in the RPE, the currents and Ca^{2+} signals elicited by heat stimulation are mediated by TRPV2 activity [22].

Like all TRP channels, TRPV2 is multimodal, and its functional importance is not solely defined by its temperature-dependent activation. TRPV2 is expressed in several tissues—for example, in endocrine organs, skeletal muscle, the heart, and the CNS [28]. These tissues normally do not show temperature changes sufficient to reach the high temperature threshold of TRPV2 (<45 °C). Here, their functional role is defined by various intracellular activation mechanisms, such as G protein-coupled receptors like those of IGF-1 [22, 31, 32] or cannabidiol (CBD) [33–36].

In the RPE, the TRPV2 channel is activated by the angiotensin II (Ang II) receptor type 1 (AT1) [33], IGF-1 receptor [22, 33], or cannabidiol receptor [22, 33]. The Ang II-dependent increase in intracellular free Ca^{2+} by TRPV2 channel activation results in a decrease in renin expression [33]. The stimulation by IGF-1 leads to increased secretion of VEGF-A [22] through TRPV2 channel activation. Since immunohistochemical analysis of choroidal neovascular membranes from patients with AMD has shown up-regulation of IGF-1 in photoreceptors and the presence of IGF-1 receptors on RPE cells, it is likely that the IGF-1-induced VEGF-A secretion via TRPV2 channel activation plays an important role in this complication, leading to rapid loss of vision [24]. Interestingly, the direct activation of TRPV2 by heat is sufficient to effect an increase in VEGF-A secretion by RPE cells [22] that is 3.5 times greater than that of untreated ARPE-19 cells.

TRPV2 channel activation, therefore, may also account for heat-evoked growth factor secretion as a mechanism for the beneficial effects of laser treatment, a common method for treating neovascularization in diabetic retinopathy, for example, where noxious heat is applied locally. There are several publications reporting altered growth factor expression after laser treatment that may be due, among other mechanisms, to heat-dependent activation of TRPV2 [13, 37–39]. Furthermore, IGF-1 also enhances surface expression of TRPV2 [31, 40], and thus IGF-1 might change the functional phenotype of the RPE, displaying higher VEGF-A secretion and higher sensitivity to secretion-stimulating factors.

In light of these observations, we investigated the regulation of TRPV2 channel activity in RPE cells. Using ARPE-19 cells as a model, we analyzed the effects of the TRPV2 channel activators CBD and IGF-1 on TRPV2 channel surface expression by means of a patch-clamp technique using confocal microscopy. We found that TRPV2 channel activity in the RPE could be stimulated both by direct channel activation and by enhancement of surface expression, and that IGF-1 and CBD differed in their respective proportions of direct channel activation and surface expression.

Materials and methods

Cell culture

The human cell line ARPE-19 (ATCC CRL-2302; American Type Culture Collection [ATCC], Manassas, VA, USA) was cultured in DMEM/F12 (Life Technologies GmbH, Darmstadt, Germany) supplemented with 10 % fetal bovine serum (FBS) and 1 % penicillin/streptomycin at 37 °C in a 5 % CO_2 atmosphere. Cells were kept serum-free for 24 h before the experiments.

For patch-clamp experiments Single cells on glass coverslips passaged to low density and grown under serum-free conditions were used for recordings 24–48 h after passaging.

For immunocytochemistry experiments Cells were grown until subconfluent under serum-free conditions and incubated with cannabidiol (15 μM: Tocris Bioscience, Wiesbaden, Germany) or IGF-1 (50 ng/ml: Thermo Fisher Scientific GmbH, Schwerte, Germany) for 10 min. LY294002 (30 μM; StressMarq Biosciences Inc., Victoria, BC, Canada) was applied for 5 min. For negative control, an equivalent amount of 1x phosphate-buffered saline (PBS) was applied. After incubation at 37 °C for 24 h, cells were fixed and subjected to immunocytochemical staining.

Immunocytochemistry of ARPE-19 cells

Cells were fixed in 4 % paraformaldehyde (PFA) for 10 min. After three washing steps using Tris-buffered saline (TBS), nonspecific antibody binding sites were blocked by incubating the cells with 5 % bovine serum albumin (BSA) in TBS. The primary antibody (rabbit polyclonal to vanilloid receptor-like protein 1 [VRL-1]; Thermo Fisher Scientific GmbH, Schwerte, Germany), diluted 1:100 in 0.8 % BSA in TBS, was applied overnight at 4 °C. The polyclonal antibody used for these experiments was specific to TRPV2, as there was not a high degree of homology between the sequences of TRPV1, 3, and 4, and the immunization peptide. After incubation with species-appropriate fluorescent-labeled secondary antibody

diluted 1:10,000 in 0.8 % BSA in TBS (goat anti-rabbit IgG-Cy3; (dianova GmbH, Hamburg, Germany) at room temperature for 1 h, cells were mounted on glass slides. The subcellular localization of TRPV2 was detected using confocal microscopy (LSM 510, Carl Zeiss GmbH, Jena, Germany) and was analyzed via the application of an edge detection algorithm in an ImageJ software program (Rasband, W.S., ImageJ, U. S. National Institutes of Health, Bethesda, Maryland, USA, http://imagej.nih.gov/ij/, 1997-2014), as previously described [41]. To calculate the relative surface expression of TRPV2, the difference between the total number of pixels in the cell (comprising the pixels in the membrane as well as the cytosol) and the number of pixels in the cytosol was divided by the total number of pixels [(∑ all pixels − ∑ pixels in the cytosol)/ ∑ all pixels].

Immunohistochemistry on paraffin sections

The eyes of adult C57BL/6 mice were fixed in 4 % PFA overnight at 4 °C and subsequently embedded in paraffin. Sections 5 μm in diameter were used for immunohistological analysis. After deparaffinization, microwave treatment, and permeabilization with 0.25 % Triton X-100 in TBS, a blocking solution (Zytomed Systems GmbH, Berlin, Germany) was applied to the slides for 60 min at room temperature. Subsequently, slides were incubated in the primary antibody (1:100; rabbit polyclonal to VRL-1, Thermo Fisher Scientific GmbH) overnight at 4 °C. After TBS wash, the slides were incubated with the fluorescent-labeled secondary antibody (1:5000, goat anti-rabbit IgG-Cy3; dianova GmbH, Hamburg, Germany). Nuclei were stained with 4',6-diamidino-2-phenylindole (DAPI). Stains were evaluated with fluorescence microscopy using an Axio Imager 2 and ZEN software (Carl Zeiss).

Patch-clamp experiments

ARPE-19 cells were placed in a bath chamber on the stage of an inverted microscope. The extracellular solution contained 130 mM NaCl, 5 mM CsCl, 2 mM $MgCl_2$, 2 mM $CaCl_2$, 10 mM HEPES, and 5 mM glucose, adjusted to pH 7.3 with NaOH. Patch-clamp electrodes with a resistance of 3–5 MΩ were pulled from borosilicate glass (DMZ-Universal Puller; Zeitz Instruments GmbH, Muenchen, Germany). The electrodes were filled with an intracellular solution containing 140 mM CsCl, 2 mM $MgCl_2$, 1 mM $CaCl_2$, 2.5 mM EGTA, and 10 mM HEPES, adjusted to pH 7.3 with CsOH. Whole-cell currents were measured with a patch-clamp amplifier (EPC-7; HEKA Elektronik Dr. Schulze GmbH, Lambrecht/Pfalz, Germany) with data acquisition and analysis software (TIDA; HEKA Elektronik). All experiments were performed at room temperature (22–25 °C). For recording of heat-induced TRPV2 currents, the bath solution was heated to 45 °C. For further characterization the channels, TRPV channel activators IGF-1 (300 ng/ml) and cannabidiol (CBD, 45 μM), the blockers ruthenium red (20 μM, Tocris) and SKF-96365 (20 μM), and the phosphatidylinositol 3-kinase (PI3K) blocker LY294002 (30 μM) were added to the bath.

Statistical analysis

Experiments were repeated at least three times. Western blots and immunohistological images shown in the figures depict a representative experiment. Values are stated as mean +/− standard error of the mean (SEM); *n* refers to the number of experiments. Statistical difference was tested using analysis of valiance (ANOVA); a statistically significant difference was considered at *p* values less than 0.05.

Results

Expression pattern of TRPV2 channels in the RPE

In situ expression of TRPV2 channels was assessed in sagittal sections of the mouse retina by means of immunohistochemistry. TRPV2 channel protein was found in the basolateral membrane of the retinal pigment epithelium (Fig. 1a and b). Furthermore, a faint staining was detected in the ganglion cell layer. Staining of the outer segments of the photoreceptors was due to nonspecific binding of the secondary antibody by the photoreceptors (1C). However, a comparison of stains by the secondary antibody either in the presence or absence of the primary antibody confirmed the RPE as an expression site for TRPV2 in the retina. In addition, cells of the human RPE cell line ARPE-19 showed TRPV2 channel protein expression with a largely intracellular localization (Fig. 1d).

Activation of TRPV2 ion channel currents in ARPE-19 cells

In order to study the mechanisms of TRPV2 channel activation, patch-clamp whole-cell recordings from ARPE-19 cells were conducted. We chose K^+-free extra- and intracellular recording conditions in order to eliminate superimposed K channel currents. The changes in membrane conductance were recorded by repeated ramping of the membrane voltage between −140 and +60 mV from a holding potential of −40 mV, which corresponds to the resting membrane potential of RPE cells [20]. In order to apply a direct and specific activation stimulus, the temperature of the bath solution was increased to 45 °C, which led to activation of membrane conductance in 60 % of the cells. The density of the current between −140 and +60 mV increased by 16.59±4.97 % (n=6; Fig. 2a–c). Forty percent of the ARPE-19 cells showed no significant change in membrane conductance (Fig. 2d). The

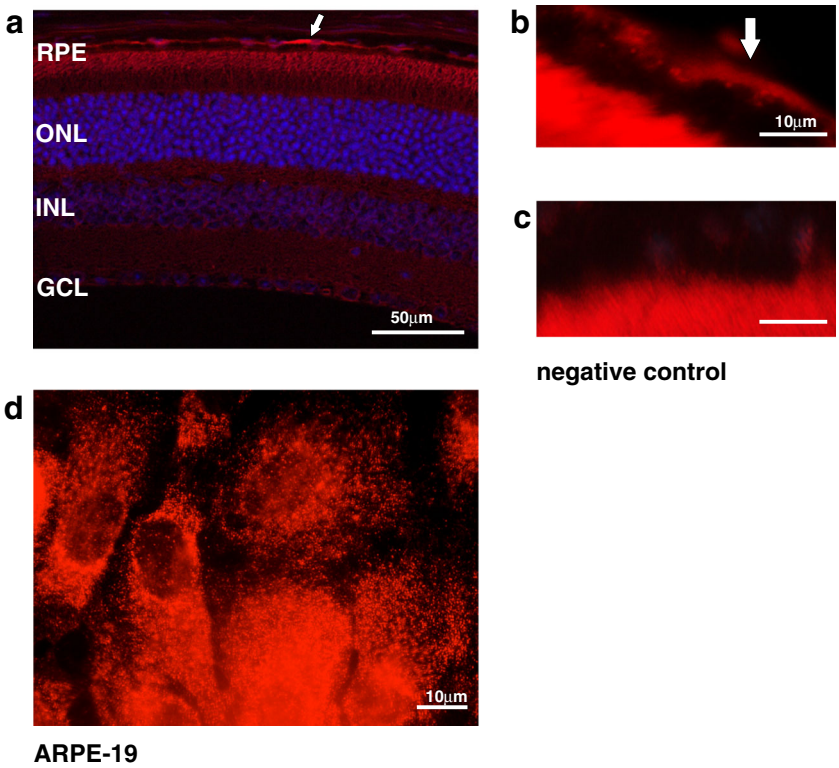

Fig. 1 Expression pattern of TRPV2 channels in the RPE. **a**–**c** Immunostaining of a deparaffinized sagittal retina section of an adult C57BL/6 mouse against TRPV2 (**a**) labeled in *red*. Nuclei were counterstained with DAPI. The *scale bar* represents 50 μm. **b** 100× magnification of the RPE of 1**a**: staining against TRPV2 revealing localization of TRPV2 in the basolateral membrane of the RPE (indicated by *white arrow*). **c** 100× magnification of a section exclusively stained with the secondary antibody revealing nonspecific staining of the photoreceptor outer segments (POS) but no signal in the RPE. The *scale bar* represents 10 μm. **d** Immunostaining of ARPE-19 cells showing endogenous expression of TRPV2 (labeled in *red*). The *scale bar* represents 10 μm. *GCL* ganglion cell layer, *INL* inner nuclear layer, *ONL* outer nuclear layer, *RPE* retinal pigment epithelium

heat-evoked membrane conductance was blocked by application of SKF-96365 (20 μM) (Fig. 2c). Thus, by means of activation temperature and blocker sensitivity, ARPE-19 cells showed functional expression of ion channels with properties of the TRPV2 channel.

In the next step, the activation of TRPV2 channels by G protein-coupled receptors was investigated. Stimulation of the cells with IGF-1 (300 ng/ml) led to a more pronounced increase in the current density, by 459±200 % (n=4), compared to that with heat alone. The IGF-1-stimulated membrane conductance could not be further stimulated by an increase in temperature (by 527±184 %; n=4, p=0.81; Fig. 3d–f). Both IGF-1-dependent and heat-dependent stimulation of membrane conductance in the presence of IGF-1 were fully blocked by SKF-96365 (−1.29±7.99 %, n=5, p=0.03; and 94± 50 %, n=5, p=0.0395, respectively; (Fig. 3f).

Comparable observations were made using CBD (45 μM) to stimulate TRPV2 channels. CBD significantly increased the current density, by 313±50 % (n=6), which was further stimulated by heat to 476±43 % (n=6, p=0.0341; Fig. 3a–c). The effects of CBD on membrane conductance were also fully blocked by application of SKF-96365 (−0.71± 6.13 %; n=4, p=0.0011 for CBD and SKF-96365; and 12.33±7.14 % n=4, p<0.001 for CBD, heat stimulation, and SKF-96365; Fig. 3c).

Regulation of surface expression of TRPV2 channels in ARPE-19 cells

IGF-1 was found to regulate the TRPV2 channel activity by increasing its surface expression via a PI3K-dependent mechanism [22, 31]. In order to test whether this mechanism applied for both the IGF-1- and CBD-dependent stimulation of TRPV2 channels in ARPE-19 cells, we used the LY294002 specific blocker of PI3K. In the presence of LY294002, neither the application of IGF-1 nor CBD resulted in a change in membrane conductance. The current density increase after application of CBD under heat stimulus to 475.73±42.97 % (n=4) decreased to 18.58±3.29 % in the presence of LY294002 (n=6, p<0.001; Fig. 5a). The same applied for IGF-1: 527.39±184.38 % (n=4) for IGF-1 under heat stimulus and 10.76±14.96 (n=5, p=0.0156) in the presence of LY294002 (Fig. 5c).

These data suggest that TRPV2 channels are activated by both IGF-1 and CBD via a PI3K-dependent mechanism. Therefore, it is possible that this occurs by direct channel

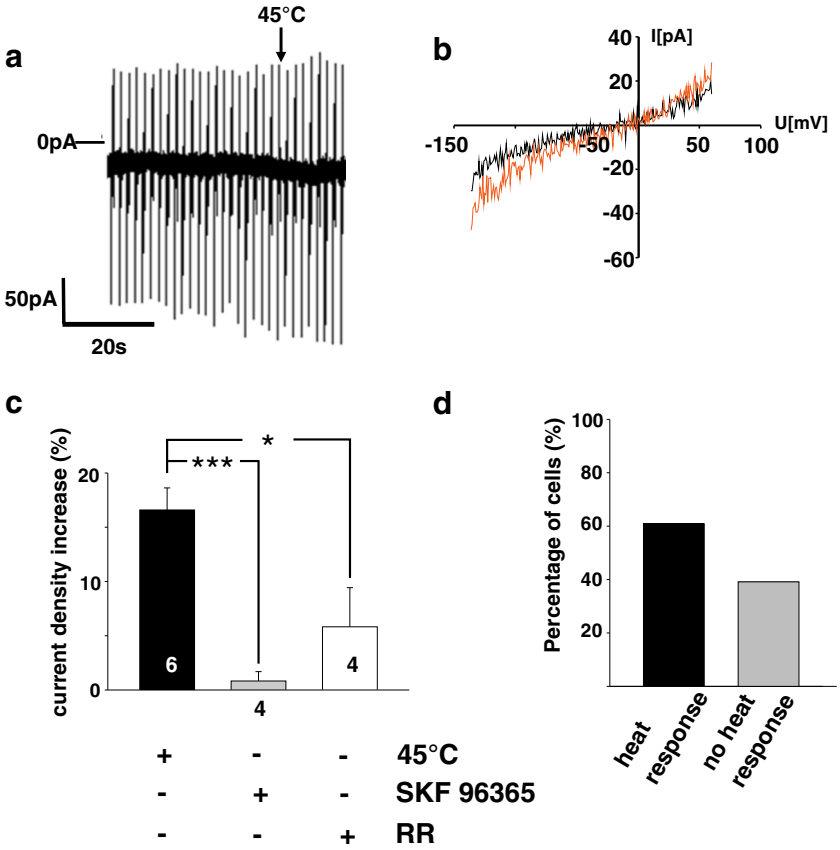

Fig. 2 Heat-induced activation of TRPV2 channels in ARPE-19 cells. **a** Raw currents through ARPE-19 cells, stimulated by repeated ramps of the membrane voltage between −140 and +60 mV from a holding potential of −40 mV, before and after increasing the temperature of the bath solution to 45 °C. **b** Current–voltage (I–U) plot of the raw currents in **a** before heat stimulation (*black line*) and during heat stimulation (*red line*), eliciting an increase of the membrane conductance. **c** *Bar chart* illustrating the percentage current density increase after heat stimulation (*black bar*) and the use of the TRPV2 blockers SKF-96365 and ruthenium red (*grey and white bars*, respectively) compared to unstimulated cells. **d** Percentage of heat-responsive and non-responsive cells: of a total of 23 cells, 14 cells showed an increase of conductance in response to a heat stimulus, whereas 9 cells showed no change in conductance. *: $p<0.05$; **$p<0.01$; ***$p<0.001$; ns not significant

activation and/or an increase in the surface expression of the TRPV2 channel protein. To test this hypothesis, we analyzed the surface expression of TRPV2 channels in ARPE-19 cells using immunohistochemistry in conjunction with confocal microscopy. The surface expression of the TRPV2 channel protein was calculated from confocal images as the ratio of TRPV2-staining-positive pixels between an outer ring around the plasma membrane and an inner ring in the cytosol after application of an edge detection tool in order to eliminate background staining, as previously described [41] (Fig. 4a–c). Using this method, we were able to show that CBD increased surface expression of the TRPV2 channel protein by around 360 %, and that IGF-1 increased surface expression by around 150 %; thus the increase was significantly less in IGF-1-treated cells than in CBD-treated cells (n=9–11; $p<0.01$ and $p < 0.001$; Fig. 4d). Since LY294002 appeared to be an efficient inhibitor of the IGF-1 or CBD-dependent stimulation of TRPV2 currents, we tested the influence of PI3K inhibition on the surface expression of TRPV2 channels. The relative surface expression mediated by IGF-1 stimulation was reduced by about 86 % (n=8–10; $p<0.001$; Fig. 5d). The same applied for CBD and LY294002 (n=9–13; $p<0.0;01$ Fig. 5b). Thus, both IGF-1 and CBD activated TRPV2 channels through increased channel activity in conjunction with increased surface expression.

Conclusions/Discussion

TRPV2 channels may be involved in the generation of pathological VEGF-A secretion. In this study, we investigated the basic mechanisms that regulate TRPV2 channel activity in the RPE. We found that TRPV2 channel activity was stimulated both by direct activation of the channel pore and by an increase in surface expression of the channel, which appeared to be regulated by PI3K.

We investigated the expression of TRPV2 channels in the retina both in situ and in vitro. In retina cross-sections of the murine eye, we found predominant expression of TRPV2

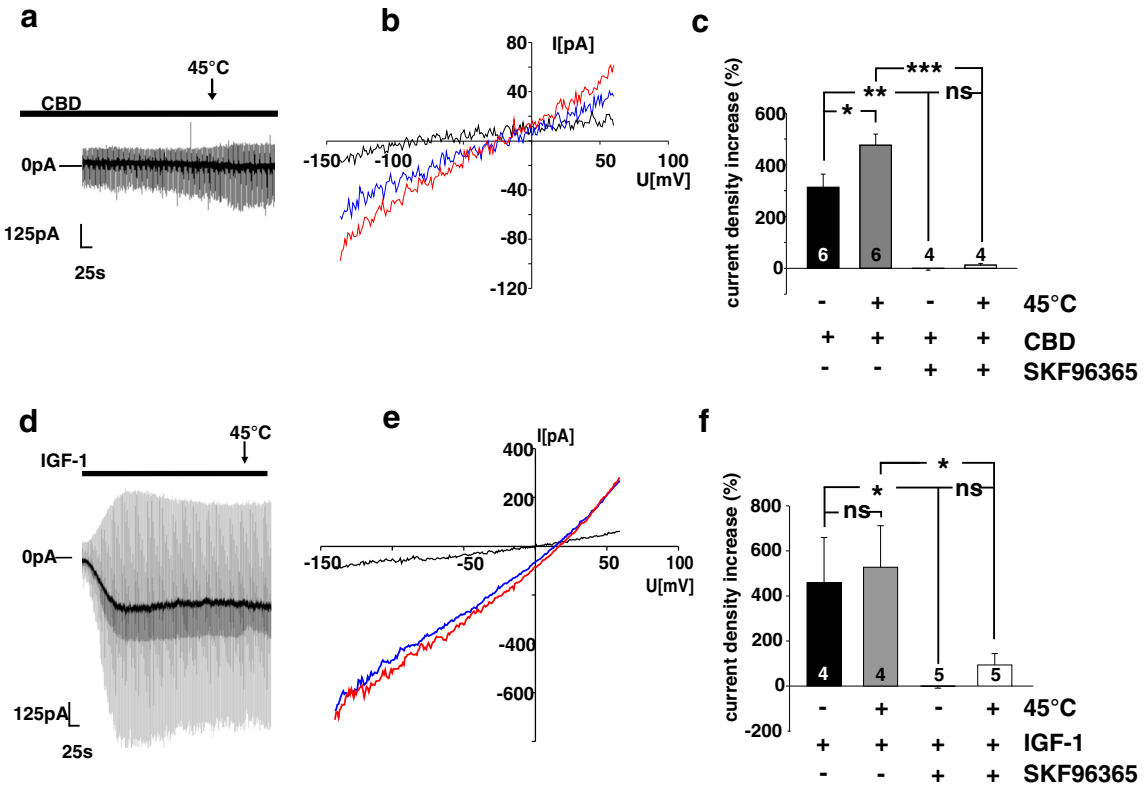

Fig. 3 G protein-induced activation of TRPV2 channels in ARPE-19 cells. **a** Raw currents through ARPE-19 cells, stimulated by repeated ramps in membrane voltage between −140 and +60 mV from a holding potential of −40 mV, in a bath solution containing CBD (45 μm), before and after increasing the temperature of the bath solution to 45 °C. **b** Current–voltage (I–U) plot of the raw currents in **a** before heat stimulation (*blue line*), during heat stimulation (*red line*), showing just an increase in membrane conductance. The *black line* represents the current–voltage relationship of control cells. **c** *Bar chart* illustrating the percentage current density increase after stimulation with the TRPV2 channel activator CBD alone (*black bar*), CBD in 45 °C hot solution (*grey bar*), CBD with the blocker SKF-96365, and CBD with SKF-96365 in the hot solution (*white bar*), compared to unstimulated cells. CBD led to a significant increase in membrane conductance, which could be further increased with heat stimulation as well as completely abolished with SKF-96365. **d–f** Same experimental design as in **a–c**, replacing CBD with another TRPV2 agonist, IGF-1. **e** Current–voltage (I–U) plot of the raw currents in **d** before heat stimulation (*blue line*) and during heat stimulation (*red line*), showing just a slight increase in outward conductance. The *black line* represents the current–voltage relationship of control cells. **f** *Bar chart* illustrating the percentage current density increase compared to unstimulated cells. Application of IGF-1 (*black bar*) led to a significant increase in membrane conductance compared to unstimulated cells, which was not able to be further increased by heat stimulation (*grey bar*) but was abolished completely by SKF-96365 (*white bar*). *: $p<0.05$; **$p<0.01$; ***$p<0.001$; ns not significant

channels in the RPE and a faint signal in the ganglion cell layer. The latter is consistent with previously published data by Leionelli et al. [42, 43]. The localization of TRPV2 in retinal sections in the RPE corresponds with the observation that cells of the RPE cell line ARPE-19 also showed expression of TRPV2 channels. Thus, functional data in human RPE cells in a primary culture, ARPE-19 cells, and mouse RPE cells in a primary culture will reflect properties of TRPV2 channel activity regulation for the native RPE [5, 22, 33]. ARPE-19 cells stained against TRPV2 channels revealed another property of these channels in the RPE. We found a large proportion of TRPV2 in the intracellular space and not in the cell membrane, which seems to be a physiological feature of these ion channels [44]. Thus the regulation of the TRPV2 channel occurs both through changes in surface expression and modulation of the pore activity.

In order to analyze the activation mechanisms of TRPV2 channels in the RPE, we used two different tools: direct channel activation by increasing the temperature to values above the activation threshold of TRPV2 channels, and with agonists known to activate TRPV2 channels via the G protein-coupled receptors IGF-1 and CBD. Among them, IGF-1 is known to act as a stimulator of TRPV2 surface expression [31, 45]. The same mechanism is discussed for CBD-dependent activation of TRPV2 microglia cells and a glioma cell line [46, 47].

In patch-clamp experiments under K^+-free conditions, increasing the temperature activated membrane conductance that was able to be completely blocked by SKF-96365 or by ruthenium red, and that showed reversal potentials indicative of a non-selective cation channel conducting both Na^+ and Ca^{2+}. Our previous work using small interfering RNA (siRNA) knockdown of TRPV2 channel expression showed that SKF-96365 predominantly blocked TRPV2 channels in the RPE [33]. Here, we found that SKF-96365 blocked the same component of increases in Ang II-dependent Ca^{2+},

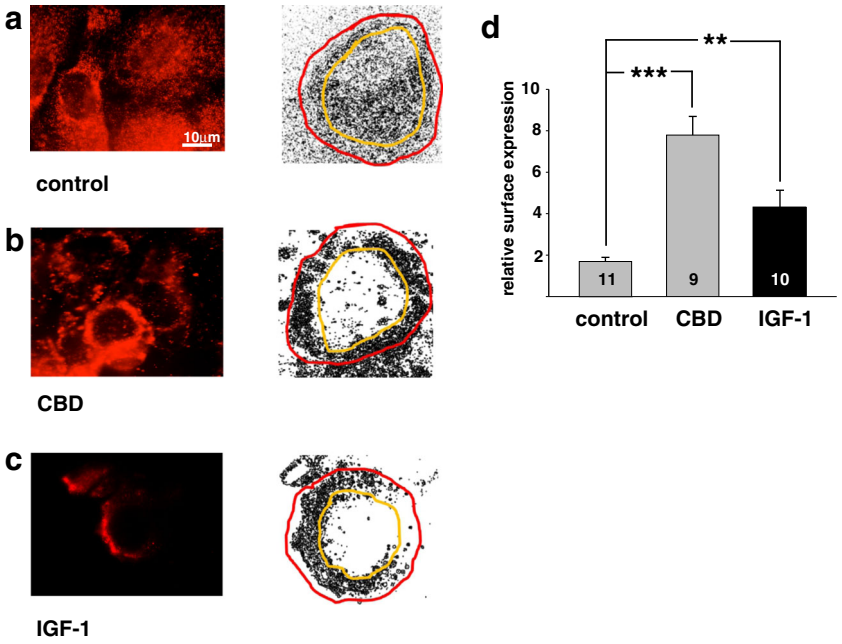

Fig. 4 G protein-induced modulation of surface expression of TRPV2 in ARPE-19 cells. **a**–**c** The *left panel* provides confocal microscopy pictures of ARPE-19 cells either unstimulated (**a**) or treated with CBD (**b**) or IGF-1 (**c**), revealing an increase in TRPV2 protein expression in the cell membrane of ARPE-19 cells after stimulation with CBD or IGF-1. The *right panel* illustrates the application of an edge detection algorithm to a single cell of the raw data on the *right panel*. The *red line* represents the outside of the cell, and the *yellow line* the inside of the cell. **d** Relative surface expression [(∑ pixels in the *red circle* – ∑ number of pixels in the *yellow circle*)/ ∑ pixels in the *red circle*] of unstimulated cells (n=11) and cells after stimulation with CBD (n=9) and IGF-1 (n=10), showing a significant increase in surface expression of the TRPV2 protein in IGF-1 and even more in CBD-stimulated cells. *: $p<0.05$; **$p<0.01$; ***$p<0.001$; ns not significant

which was also reduced by siRNA knockdown. Taken together, these data suggest that heat-activated membrane conductance can be identified as an activity of TRPV2 channels. The fact that only 60 % of the cells showed a heat response is most likely due to specialization of RPE cells within the monolayer. Whereas all RPE cells contribute to basic functions such as epithelial transport of nutrients and water, visual cycle, and phagocytosis [5], there are certain RPE cells specialized for other functions such as secretion—for example, growth factors on one hand and immune regulators on the other—and the underlying pathways require specialized protein expression. Such specialization may explain the fact that not all cells express TRPV2 channels. We observed this phenomenon in terms of complement signaling, which we reported in a recent publication [48].

IGF-1 and CBD led to a much greater increase in membrane conductance than heat stimulation alone, and the effects of both IGF-1 and CBD were again blocked by SKF-96563. Therefore, IGF-1 and CBD are also involved in activation of TRPV2 channels in the RPE. Quantitative immunocytochemical analysis revealed a mechanism by which IGF-1 and CBD more strongly activated TRPV2 channel currents than heat alone. Similar to that in non-stimulated cells, TRPV2 staining was more prominent in the cytoplasm; this pattern evolved into one in which TRPV2 localization was significantly increased in the plasma membrane after stimulation with either IGF-1 or CBD. Therefore, the increase of TRPV2 conductance in ARPE-19 cells by CBD and IGF-1 involves an increase in surface expression of TRPV2. Using LY294002 that abolished the increase in membrane conductance and surface expression by IGF-1 and CBD, we were able to demonstrate that the effects of these agonists underlie a PI3K-dependent modulation of TRPV2, a mechanism that was also demonstrated by Link et al. [49]. In summary, the tools selected for this study are suitable for analyzing the two basic TRPV2 channel activation mechanisms in RPE cells: stimulation of pore activity and increased surface expression.

The investigation of TRPV2-activating effects revealed marked differences between the two agonists. The increase in TRPV2 surface expression was significantly lower with IGF-1 than with CBD, whereas IGF-1 led to a stronger increase in membrane conductance, which could not be further stimulated by heat. Thus it is evident that the TRPV2 stimulating mechanism of IGF-1 is based on both increased surface expression and stimulation of the channel activity itself, such that a physiological heat stimulus cannot further increase membrane conductance. CBD, on the other hand, primarily stimulates surface expression of TRPV2, with a weaker effect on the membrane conductance, but it can be further stimulated by heat. As such, regulation of TRPV2 channel activity includes both surface expression and channel activation. The two agonists use different proportions of the activation

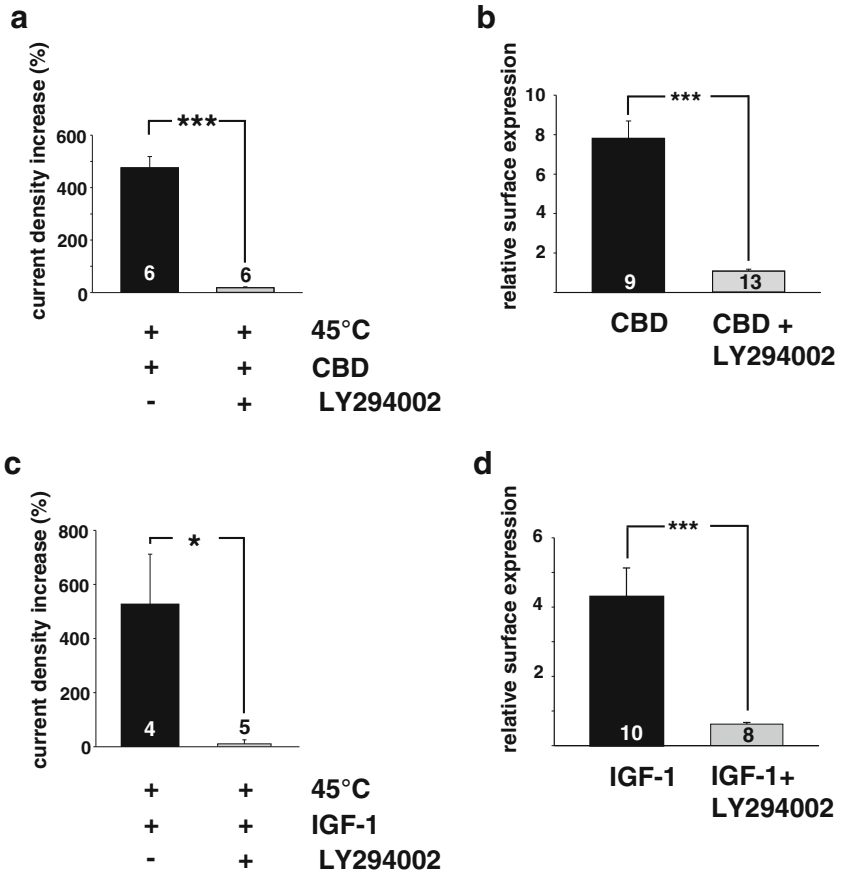

Fig. 5 Effect of PI 3-kinase (PI3K) inhibition on the activation of TRPV2. **a** *Bar chart* illustrating the percentage current density increase compared to unstimulated cells. Application of LY294002 (*grey bar*) led to a significant decrease in current density compared to CBD- and heat-stimulated cells (*black bar*) **b** Relative surface expression of CBD-stimulated cells (n=9) and cells stimulated with CBD in the presence of LY294002 (n=13), showing a significant reduction in surface expression of TRPV2 protein with PI3K inhibition. **c** *Bar chart* illustrating the percentage current density increase compared to unstimulated cells. Application of LY294002 (*grey bar*) led to a significant decrease in current density compared to IGF-1- and heat-stimulated cells (*black bar*). **d** Relative surface expression of IGF-1-stimulated cells (n=10) and cells stimulated with CBD in the presence of LY294002 (n=8), showing a significant decrease in surface expression of TRPV2 protein with PI3K inhibition.

mechanisms to fine-tune the resulting increase in membrane conductance and corresponding Ca^{2+} signals.

Interestingly, although one would have expected a slower time course for increases in surface expression, there was no difference in time course between direct activation by channel phosphorylation and increased surface expression. The increase in surface expression, however, does not require de novo protein production. As can be seen in the confocal images, the protein is already available and must only be translocated into the cell membrane upon stimulation. This can occur in a very short period of time, as is observable in a variety of ion channels that provide increased membrane conductance by increased surface expression as well as for TRPV2 [49]—within minutes.

In the RPE, the dual TRPV2 activation by heat and surface expression is of interest in the context of laser treatment, a method routinely used not only in ophthalmology but in basic animal research as well. In basic research, photocoagulation of the retina in animals, predominantly mice, is an established model for inducing choroidal neovascularization [50, 51], a major complication of AMD [7, 16, 52]. In these models, laser photocoagulation causes a rupture of Bruch's membrane and subsequent outgrowth of choroidal vessels into the retina, driven by VEGF-A [12, 52–54]. Since the RPE is a major source of VEGF-A [5, 12, 16, 54], which is secreted under the control of TRPV2 channels [22], our findings would imply that there are two pathways regulating VEGF-A secretion by the RPE: by directly increasing the temperature of the retinal tissue and via IGF-1, which is known to stimulate VEGF-A secretion [24–26, 55] in a PI3K-dependent manner [22]. As it is known that the therapeutic impact of laser treatment also results from an increase in the secretion of a variety of growth factors [22, 39], it is likely that the secretion of a portion of them is directly controlled by heat. The mechanisms explored in this study reveal that heat sensitivity of RPE cells can be specifically modulated depending on various factors, some of them known to be involved in the pathology of retinal degeneration such as AMD or diabetic retinopathy. A further

understanding of these factors and their correlation with specific disease stages will open new avenues for development of therapeutic strategies in laser treatment defined by the heat sensitivity of the RPE.

Acknowledgments The authors thank PD Dr. Rita Rosenthal, Institute for Clinical Physiology, Charité University Medicine Berlin, for providing access to the confocal microscope.

References

1. Bok D (1993) The retinal pigment epithelium: a versatile partner in vision. J Cell Sci Suppl 17:189–195
2. Marmorstein AD (2001) The polarity of the retinal pigment epithelium. Traffic 2:867–872
3. Rizzolo LJ (1997) Polarity and the development of the outer blood-retinal barrier. Histol Histopathol 12:1057–1067
4. Steinberg RH (1985) Interactions between the retinal pigment epithelium and the neural retina. Doc Ophthalmol 60:327–346
5. Strauss O (2005) The retinal pigment epithelium in visual function. Physiol Rev 85:845–881. doi:10.1152/physrev.00021.2004
6. Nowak JZ (2006) Age-related macular degeneration (AMD): pathogenesis and therapy. Pharmacol Rep 58:353–363
7. Zarbin MA (1998) Age-related macular degeneration: review of pathogenesis. Eur J Ophthalmol 8:199–206
8. Phelan JK, Bok D (2000) A brief review of retinitis pigmentosa and the identified retinitis pigmentosa genes. Mol Vis 6:116–124
9. van Soest S, Westerveld A, de Jong PT, Bleeker-Wagemakers EM, Bergen AA (1999) Retinitis pigmentosa: defined from a molecular point of view. Surv Ophthalmol 43:321–334
10. Burns MS, Hartz MJ (1992) The retinal pigment epithelium induces fenestration of endothelial cells in vivo. Curr Eye Res 11:863–873
11. Roberts WG, Palade GE (1995) Increased microvascular permeability and endothelial fenestration induced by vascular endothelial growth factor. J Cell Sci 108(Pt 6):2369–2379
12. Witmer AN, Vrensen GF, Van Noorden CJ, Schlingemann RO (2003) Vascular endothelial growth factors and angiogenesis in eye disease. Prog Retin Eye Res 22:1–29
13. Ogata N, Wada M, Otsuji T, Jo N, Tombran-Tink J, Matsumura M (2002) Expression of pigment epithelium-derived factor in normal adult rat eye and experimental choroidal neovascularization. Invest Ophthalmol Vis Sci 43:1168–1175
14. Ogata N, Wang L, Jo N, Tombran-Tink J, Takahashi K, Mrazek D, Matsumura M (2001) Pigment epithelium derived factor as a neuroprotective agent against ischemic retinal injury. Curr Eye Res 22: 245–252
15. Steele FR, Chader GJ, Johnson LV, Tombran-Tink J (1993) Pigment epithelium-derived factor: neurotrophic activity and identification as a member of the serine protease inhibitor gene family. Proc Natl Acad Sci U S A 90:1526–1530
16. Strauss O, Heimann H, Foerster M, Agostini H, Hansen L, Rosenthal R (2003) Activation of L-type Ca2+ channels is necessary for growth factor-dependent stimulation of VEGF secretion by RPE cells. Investig Ophtalmol Vis Sci 44:3926
17. Campochiaro PA (2000) Retinal and choroidal neovascularization. J Cell Physiol 184:301–310. doi:10.1002/1097-4652(200009)184:3<301::AID-JCP3>3.0.CO;2-H
18. Rosenthal R, Malek G, Salomon N, Peill-Meininghaus M, Coeppicus L, Wohlleben H, Wimmers S, Bowes Rickman C, Strauss O (2005) The fibroblast growth factor receptors, FGFR-1 and FGFR-2, mediate two independent signalling pathways in human retinal pigment epithelial cells. Biochem Biophys Res Commun 337:241–247. doi:10.1016/j.bbrc.2005.09.028
19. Rosenthal R, Heimann H, Agostini H, Martin G, Hansen LL, Strauss O (2007) Ca2+ channels in retinal pigment epithelial cells regulate vascular endothelial growth factor secretion rates in health and disease. Mol Vis 13:443–456
20. Reichhart N, Strauss O (2014) Ion channels and transporters of the retinal pigment epithelium. Exp Eye Res 126:27–37. doi:10.1016/j.exer.2014.05.005
21. Boulton ME, Cai J, Grant MB (2008) Gamma-secretase: a multifaceted regulator of angiogenesis. J Cell Mol Med 12:781–795. doi:10.1111/j.1582-4934.2008.00274.x
22. Cordeiro S, Seyler S, Stindl J, Milenkovic VM, Strauss O (2010) Heat-sensitive TRPV channels in retinal pigment epithelial cells: regulation of VEGF-A secretion. Invest Ophthalmol Vis Sci 51:6001–6008. doi:10.1167/iovs. 09-4720
23. Punglia RS, Lu M, Hsu J, Kuroki M, Tolentino MJ, Keough K, Levy AP, Levy NS, Goldberg MA, D'Amato RJ, Adamis AP (1997) Regulation of vascular endothelial growth factor expression by insulin-like growth factor I. Diabetes 46:1619–1626
24. Rosenthal R, Wohlleben H, Malek G, Schlichting L, Thieme H, Bowes Rickman C, Strauss O (2004) Insulin-like growth factor-1 contributes to neovascularization in age-related macular degeneration. Biochem Biophys Res Commun 323:1203–1208. doi:10.1016/j.bbrc.2004.08.219
25. Slomiany MG, Rosenzweig SA (2004) IGF-1-induced VEGF and IGFBP-3 secretion correlates with increased HIF-1 alpha expression and activity in retinal pigment epithelial cell line D407. Invest Ophthalmol Vis Sci 45:2838–2847. doi:10.1167/iovs. 03-0565
26. Slomiany MG, Rosenzweig SA (2004) Autocrine effects of IGF-I-induced VEGF and IGFBP-3 secretion in retinal pigment epithelial cell line ARPE-19. Am J Physiol Cell Physiol 287:C746–C753. doi:10.1152/ajpcell.00568.2003
27. Rosenthal R, Strauss O (2002) Ca2+−channels in the RPE. Adv Exp Med Biol 514:225–235
28. Peralvarez-Marin A, Donate-Macian P, Gaudet R (2013) What do we know about the transient receptor potential vanilloid 2 (TRPV2) ion channel? FEBS J 280:5471–5487. doi:10.1111/febs.12302
29. Tominaga M, Caterina MJ (2004) Thermosensation and pain. J Neurobiol 61:3–12. doi:10.1002/neu.20079
30. Vriens J, Appendino G, Nilius B (2009) Pharmacology of vanilloid transient receptor potential cation channels. Mol Pharmacol 75:1262–1279. doi:10.1124/mol.109.055624
31. Kanzaki M, Zhang YQ, Mashima H, Li L, Shibata H, Kojima I (1999) Translocation of a calcium-permeable cation channel induced by insulin-like growth factor-I. Nat Cell Biol 1:165–170. doi:10.1038/11086
32. Kojima I, Nagasawa M (2007) TRPV2: A calcium-permeable cation channel regulated by insulin-like growth factors. In: Liedtke WB, Heller S (eds) TRP ion channel function in sensory transduction and cellular signaling cascades, Boca Raton (FL)
33. Barro-Soria R, Stindl J, Muller C, Foeckler R, Todorov V, Castrop H, Strauss O (2012) Angiotensin-2-mediated Ca2+ signaling in the retinal pigment epithelium: role of angiotensin-receptor-associated-protein and TRPV2 channel. PLoS One 7:e49624. doi:10.1371/journal.pone.0049624
34. De Petrocellis L, Ligresti A, Moriello AS, Allara M, Bisogno T, Petrosino S, Stott CG, Di Marzo V (2011) Effects of cannabinoids and cannabinoid-enriched Cannabis extracts on TRP channels and endocannabinoid metabolic enzymes. Br J Pharmacol 163:1479–1494. doi:10.1111/j.1476-5381.2010.01166.x
35. Hegde VL, Nagarkatti PS, Nagarkatti M (2011) Role of myeloid-derived suppressor cells in amelioration of experimental autoimmune hepatitis following activation of TRPV1 receptors by cannabidiol. PLoS One 6:e18281. doi:10.1371/journal.pone.0018281

36. Qin N, Neeper MP, Liu Y, Hutchinson TL, Lubin ML, Flores CM (2008) TRPV2 is activated by cannabidiol and mediates CGRP release in cultured rat dorsal root ganglion neurons. J Neurosci 28: 6231–6238. doi:10.1523/JNEUROSCI. 0504-08.2008
37. Flaxel C, Bradle J, Acott T, Samples JR (2007) Retinal pigment epithelium produces matrix metalloproteinases after laser treatment. Retina 27:629–634. doi:10.1097/01.iae.0000249561.02567.fd
38. Hattenbach LO, Beck KF, Pfeilschifter J, Koch F, Ohrloff C, Schacke W (2005) Pigment-epithelium-derived factor is upregulated in photocoagulated human retinal pigment epithelial cells. Ophthalmic Res 37:341–346. doi:10.1159/000088263
39. Faby H, Hillenkamp J, Roider J, Klettner A (2014) Hyperthermia-induced upregulation of vascular endothelial growth factor in retinal pigment epithelial cells is regulated by mitogen-activated protein kinases. Graefes Arch Clin Exp Ophthalmol = Albrecht Graefes Arch Klin Exp Ophthalmol. doi:10.1007/s00417-014-2750-z
40. Hassan S, Eldeeb K, Millns P, Bennett A, Alexander S, Kendall D (2014) Cannabidiol enhances microglial phagocytosis via transient receptor potential (TRP) channel activation. Br J Pharmacol. doi:10.1111/bph.12615
41. Milenkovic VM, Krejcova S, Reichhart N, Wagner A, Strauss O (2011) Interaction of bestrophin-1 and Ca2+ channel beta-subunits: identification of new binding domains on the bestrophin-1 C-terminus. PLoS One 6:e19364. doi:10.1371/journal.pone.0019364
42. Yazulla S, Studholme KM (2004) Vanilloid receptor like 1 (VRL1) immunoreactivity in mammalian retina: colocalization with somatostatin and purinergic P2X1 receptors. J Comp Neurol 474:407–418. doi:10.1002/cne.20144
43. Leonelli M, Martins DO, Kihara AH, Britto LR (2009) Ontogenetic expression of the vanilloid receptors TRPV1 and TRPV2 in the rat retina. Int J Dev Neurosci : Off J Intl Soc Dev Neurosci 27:709–718. doi:10.1016/j.ijdevneu.2009.07.003
44. Gees M, Colsoul B, Nilius B (2010) The role of transient receptor potential cation channels in Ca2+ signaling. Cold Spring Harb Perspect Biol 2:a003962. doi:10.1101/cshperspect.a003962
45. Gailly P (2012) TRP channels in normal and dystrophic skeletal muscle. Curr Opin Pharmacol 12:326–334. doi:10.1016/j.coph.2012.01.018
46. Hassan S, Eldeeb K, Millns PJ, Bennett AJ, Alexander SP, Kendall DA (2014) Cannabidiol enhances microglial phagocytosis via transient receptor potential (TRP) channel activation. Br J Pharmacol 171:2426–2439. doi:10.1111/bph.12615
47. Nabissi M, Morelli MB, Santoni M, Santoni G (2013) Triggering of the TRPV2 channel by cannabidiol sensitizes glioblastoma cells to cytotoxic chemotherapeutic agents. Carcinogenesis 34:48–57. doi:10.1093/carcin/bgs328
48. Genewsky A, Jost I, Busch C, Huber C, Stindl J, Skerka C, Zipfel PF, Rohrer B, Strauss O (2014) Activation of endogenously expressed ion channels by active complement in the retinal pigment epithelium. Pflugers Arch - Eur J Physiol. doi:10.1007/s00424-014-1656-2
49. Link TM, Park U, Vonakis BM, Raben DM, Soloski MJ, Caterina MJ (2010) TRPV2 has a pivotal role in macrophage particle binding and phagocytosis. Nat Immunol 11:232–239. doi:10.1038/ni.1842
50. Grossniklaus HE, Kang SJ, Berglin L (2010) Animal models of choroidal and retinal neovascularization. Prog Retin Eye Res 29:500–519. doi:10.1016/j.preteyeres.2010.05.003
51. Tobe T, Ortega S, Luna JD, Ozaki H, Okamoto N, Derevjanik NL, Vinores SA, Basilico C, Campochiaro PA (1998) Targeted disruption of the FGF2 gene does not prevent choroidal neovascularization in a murine model. Am J Pathol 153:1641–1646. doi:10.1016/S0002-9440(10)65753-7
52. Campochiaro PA, Soloway P, Ryan SJ, Miller JW (1999) The pathogenesis of choroidal neovascularization in patients with age-related macular degeneration. Mol Vis 5:34
53. Ishibashi T, Hata Y, Yoshikawa H, Nakagawa K, Sueishi K, Inomata H (1997) Expression of vascular endothelial growth factor in experimental choroidal neovascularization. Graefes Arch Clin Exp Ophthalmol = Albrecht Graefes Arch Klin Exp Ophthalmol 235: 159–167
54. Schlingemann RO (2004) Role of growth factors and the wound healing response in age-related macular degeneration. Graefes Arch Clin Exp Ophthalmol = Albrecht Graefes Arch Klin Exp Ophthalmol 242:91–101. doi:10.1007/s00417-003-0828-0
55. Smith LE, Shen W, Perruzzi C, Soker S, Kinose F, Xu X, Robinson G, Driver S, Bischoff J, Zhang B, Schaeffer JM, Senger DR (1999) Regulation of vascular endothelial growth factor-dependent retinal neovascularization by insulin-like growth factor-1 receptor. Nat Med 5:1390–1395. doi:10.1038/70963